

Type-1 and type-2 fuzzy logic-based space vector modulation for two-level inverter fed induction motor

Abhiram Tikkani¹, Polaki V. N. Prasad²

¹Department of Electrical and Electronics Engineering, Sreenidhi Institute of Science and Technology, Hyderabad, India

²Department of Electrical Engineering, University College of Engineering, Osmania University, Hyderabad, India

Article Info

Article history:

Received Mar 05, 2021

Revised May 30, 2022

Accepted Jun 08, 2022

Keywords:

Induction motor

Pulse width modulation

Space vector modulation

Type-1 fuzzy logic

Type-2 fuzzy logic

ABSTRACT

Two-level inverter control with type-1 and type-2 fuzzy logic-based space vector pulse-width modulation (PWM) method for induction motor drive (IMD) is presented in this paper. A new sampling time independent strategy with type-1 and type-2 fuzzy based methods are used in generating three phase duty ratios which are directly obtained without mathematical equations. The conventional method of space vector modulation (SVM) produces the duty ratios for the inverter which are sampling time dependent. However, in type-1 and type-2 fuzzy based space vector PWM algorithms, the three phases duty ratios generated are sampling time independent and with a new integrated dead-time insertion in SVM itself, can be implemented practically for any switching frequency. As the rule-base for Mamdani non-singleton interval type-1 and type-2 fuzzy inference systems are designed manually, with the expert knowledge of conventional space vector PWM, the duty ratios of the inverter are generated such that the performance of the IMD is improved. The simulation studies for aforementioned cases is performed in matrix laboratory (MATLAB) and experimental validation for the proposed space vector PWM algorithms is validated using real-time sacraetheologiae magister (STM) hardware with STM32F429I Cortex M4 processor for a 1 hp IMD.

This is an open access article under the [CC BY-SA](https://creativecommons.org/licenses/by-sa/4.0/) license.



Corresponding Author:

Abhiram Tikkani

Department of Electrical and Electronics Engineering

Sreenidhi Institute of Science and Technology, Hyderabad, India

Email: abhiram.cbz@gmail.com

1. INTRODUCTION

Artificial intelligence is a group of methodology whose fundamental nature is to use the extensive ambiguity of the real-world tolerance, imprecision, and partial truth to realize tractability, robustness, low solution cost, and better understanding with certainty. In complex system, there are problems of incompetence to build mathematical model for the problem as problems are described by huge quantities of data that are used in studies. Usually, an expert system has an inference engine to manage the user interface, peripheral files, program files, program access and planning. Secondly, a knowledge base which comprises the information specific to a particular problem permitting an expert to define rules which regulate a process. genetic algorithms (GA) are search algorithms based on the mechanics of natural selection and natural genetics. GA operate by searching from a population of points but not a single point. The operation of GA is to quest from a population of data points with aid of objective function information using probabilistic transition rules. Particle swarm optimization (PSO) proposed in [1] is inspired by birds flocking. It is a

simple algorithm, easy to implement and has few adjustable parameters. Algorithm begins with population of particles. Each particle is improved by adjusting their velocity based on their own best over iterations (pbest) and over all best of all particles (gbest). This method has been used to solve the non-linear equations of the selective harmonic elimination (SHE) based pulse-width modulation (PWM) and to find the best switching angles. The comparative evaluation with various soft computing methods with respect to convergence and number of iterations is shown in Figure 1(a). Figure 1(b) shows comparative evaluation with complexity and popularity.

Biogeography based optimization (BBO) proposed in [2] is based on study of geographical distribution of biological organisms. Two vital facets of this method are habitat suitability index which considers the geography-based suitability of islands for habitation and suitability index variables including habitability related features such as rainfall, topography, diversity of vegetation, and temperature. Bee algorithm (BA) given in [3], [4] applied SHE is based on food foraging behavior of honey bees. Bacterial foraging algorithm (BFA) consists of four stages which includes chemotaxis (swimming and tumbling), swarming, reproduction, and dispersal. It is based on the natural characteristic of accepting the talent living creature in terms of food searching capability as survival being. This process consists of four steps. The first step is known as chemotaxis as in [5], [6]. With the evolution of population, the difference between each individual value decreases which influences the convergence speed to reach optimum value [7], [8]. The flow of differential evolution's generate-and-test loop mechanism [9] of clone in immune system explored in the field of artificial intelligence is the basis of clonal search algorithm (CSA). A brief performance evaluation of algorithms applied for SHE method for inverter control is described in [1]. Deterministic rule-based systems particularly, soft computing-based techniques such as artificial neural network (ANN) based space vector modulation (SVM) and adaptive neuro-fuzzy (ANF) based SVM fed induction motor drive (IMD) have been reported in the literature in good detail [10], [11]. The incorporation of fuzzy logic controllers (FLCs) in closed loop operation of adjustable speed drives as an improved alternative over conventional proportional integral (PI) controllers is already established in [12]-[14]. Hybrid real coded genetic algorithm pattern search (HRGA-PS) has advantage of reduced computational burden, faster convergence rate and higher probability of finding global optima [15], [16]. In [16] continuous genetic algorithm is used to compute switching angles and produce less total harmonic distortion (THD).

The PSO algorithm is provided in [17], [18]. Ant colony system (ACS) used in eliminating harmonics in PWM is based on foraging behaviour of colony of ants [19]. Food searching process of ant is replicated in ACS. Ants are used to deposit a special substance called "pheromone" [19], [20] in their path of food searching. Higher pheromone content enhances greater probability of finding food along the path. This path also helps to incur other ants to the path. Visited location and pheromone content is stored in tabu list [20]. Ants move as per the value of pheromone content and movement probability. The movement probability higher than a threshold value represents that the ant is in more favourable region [20].

In this research paper, the performance of the two-level inverter fed induction motor drive has been evaluated for inverter's source side performance in terms of overall efficiency of IMD. Also on the load side of the inverter, the performance is evaluated in terms of THD of line voltage and stator current of induction motor (IM) drive. The steady state torque ripple load conditions is also evaluated. To generate the duty ratios of the inverter, type-1 and type-2 FLCs with centroid de-fuzzification method which is suitable amongst centre of sets type, centre of heights type and centre of sum type methods. The proposed type-1 and type-2 fuzzy based SVM is verified through real-time sacrae theologiae magister (STM) hardware.

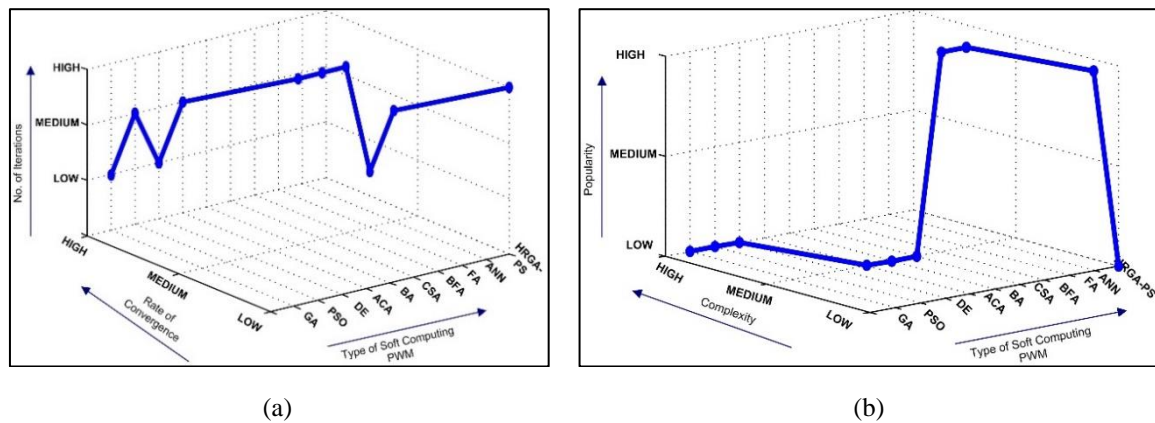


Figure 1. Comparison of soft computing based PWM methods based on: (a) convergence and (b) complexity

A comprehensive detailed matrix laboratory (MATLAB) simulation and real-time results are described to support the feasibility of proposed control strategy. To support the claims of type-1 and type-2 fuzzy logic based SVM algorithms, performance is evaluated and compared with literature reported conventional SVM method of the two-level inverter fed IMD. The experimentation is done on an advanced RISC machine (ARM) cortex M4 processor is a new version of reduced instruction set computer (RISC) based processor for implementation of proposed SVM algorithms which generates gate pulses for IMD.

2. RESEARCH METHOD

The block diagram of SVM algorithm is described in Figure 2, which is implemented for a two-level inverter fed IMD shown in Figure 3(a) and Figure 3(b). The eight possible switching states from [- - -] to [+ + +] for the power inverter forming the eight edges of space vector diagram is shown in Table 1. The main function of space vector modulation is to produce three sinusoidal currents so that air gap flux has circular tracking path. Hence, stator mmf is resolved as in (1) resulting in current space phasor in (2) and reference voltage space vector in (3).

$$N_s \vec{I}_s = N_s i_\alpha + j N_s i_\beta \quad (1)$$

$$\vec{I}_s = i_\alpha + j \cdot i_\beta \quad (2)$$

$$\vec{V}_{ref} = v_\alpha + j v_\beta \quad (3)$$

The resulting reference voltage space vector is expressed in polar form as in (4) which is obtained from three phase reference voltages as given in (5) and (6).

$$\vec{V}_{ref} = |\vec{V}_{ref}| \cdot e^{j\theta} \quad (4)$$

$$v_\alpha = 1.5 \cdot \overline{V_{an}}, v_\beta = j0.866 \cdot (\overline{V_{bn}} - \overline{V_{cn}}) \quad (5)$$

$$|\vec{V}_{ref}| = \sqrt{v_\alpha^2 + v_\beta^2}, \theta = \tan^{-1} \left(\frac{v_\beta}{v_\alpha} \right) \quad (6)$$

The reference voltage space vector is generated using principle of volt-second balancing. Corresponding dwelling times are calculated and the duty cycles d_{t1} , d_{t2} , and d_{t0} are obtained from (7) to (9). The null time duty ratio is given in (9) and relationship between sector angle β given in (10) and duty cycle is derived from phase angle θ using (6).

$$d_{t1} = 1.155 \left(\frac{|\vec{V}_{ref}|}{V_{dc}} \right) \sin(60 - \beta) \quad (7)$$

$$d_{t2} = 1.155 \left(\frac{|\vec{V}_{ref}|}{V_{dc}} \right) \sin(\beta) \quad (8)$$

$$d_{t0} = 1 - (d_{t1} + d_{t2}) \quad (9)$$

$$\beta = \left(\frac{n\pi}{3} - \theta \right) \quad (10)$$

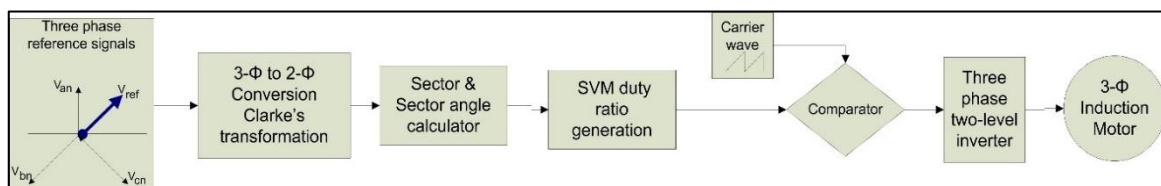


Figure 2. Block diagram for implementing SVM

Table 1. Switching states and voltages of two-level inverter

No	State	Vab	Vbc	Vca	Van	Vbn	Vcn
1	+- -	V _{dc}	0	-V _{dc}	2V _{dc} /3	-V _{dc} /3	-V _{dc} /3
2	+++	0	V _{dc}	-V _{dc}	-V _{dc} /3	+V _{dc} /3	-2V _{dc} /3
3	-+ -	-V _{dc}	V _{dc}	0	-V _{dc} /3	2V _{dc} /3	-V _{dc} /3
4	-++	-V _{dc}	0	V _{dc}	-2V _{dc} /3	V _{dc} /3	V _{dc} /3
5	-- +	0	-V _{dc}	V _{dc}	-V _{dc} /3	-V _{dc} /3	2V _{dc} /3
6	+++	V _{dc}	-V _{dc}	0	V _{dc} /3	-2V _{dc} /3	V _{dc} /3
7	+++	V _{dc}	V _{dc}	V _{dc}	0	0	0
8	- - -	0	0	0	0	0	0

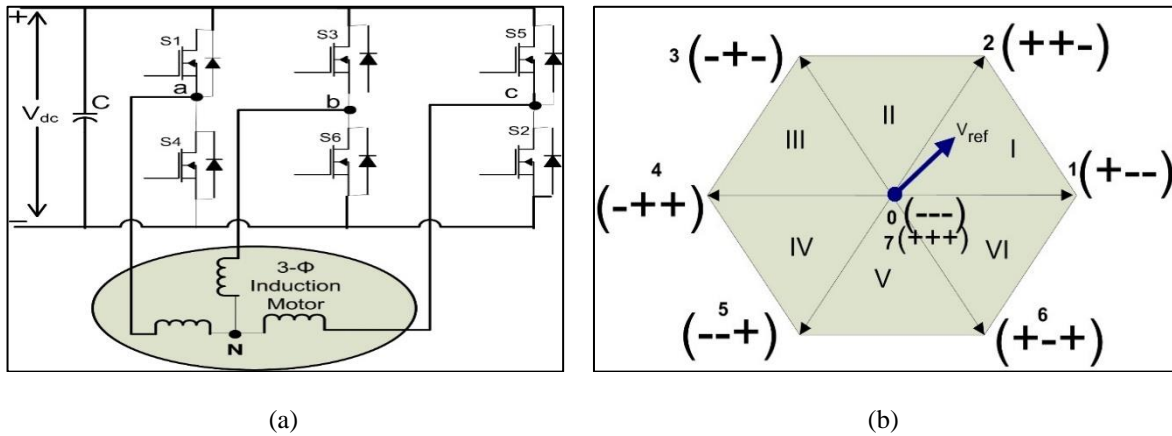


Figure 3 Two-level inverter fed IMD: (a) two-level VSI fed IM and (b) space vector diagram

The obtained dwell time duty cycles are applied in a sequential manner for each sector ($n = 1$ to 6) as given in Figure 4(a) representing gate pulse pattern. The three phase duty ratios generation is shown in Figure 4(b). Based on switching states given in Table 1, for a given sampling time $T_s = 2T_Z$ shown in (11), the instantaneous average phase voltages $[V_{anav} V_{bnav} V_{cnav}]$ are obtained for sector 1 as in (12) to (14) respectively. These instantaneous average phase voltages are developed for each interval of sample time and are calculated for reference voltage vector which are discussed in section 3. The integrated dead time insertion in SVM is incorporated as in [21]. From (7) to (9), duty ratios $d_{t1} = T_1/T_Z$, $d_{t2} = T_2/T_Z$ which are varying for each sample of reference voltage vector.

$$T_Z = 1 - (T_1 + T_2) = T_s/2 \tag{11}$$

$$V_{anav} = \left(\frac{2V_{dc}}{3}\right) d_{t1} + \left(\frac{V_{dc}}{3}\right) d_{t2} \tag{12}$$

$$V_{bnav} = \left(\frac{2V_{dc}}{3}\right) d_{t1} + \left(\frac{V_{dc}}{3}\right) d_{t2} \tag{13}$$

$$V_{cnav} = \left(\frac{2V_{dc}}{3}\right) d_{t1} + \left(\frac{V_{dc}}{3}\right) d_{t2} \tag{14}$$

2.1. Proposed fuzzy logic-based space vector PWM

The input-output mapping is processed through a if-then rule base for a fuzzy system. In Figure 5(a) the architecture and description of type-1 and in Figure 5(b) architecture and description of type-2 fuzzy system is depicted. The benefits of type-2 fuzzy logic controller (T2FLC) over type-1 fuzzy logic controller (T1FLC) are given in [22], [23]. However, dead time can be inserted as in [24] in PWM algorithms of [22], [23]. The complete fuzzy computing method has background concept of fuzzy set theory [25]-[29]. One of the key benefits with T2FLC over T1FLC is that each membership function of T2FLC has foot print of uncertainty (FOU) which by far can better handle linguistic and numerical ambiguities related with the inputs and/or outputs of the fuzzy inference system. Type reduction is an additional step after defuzzification in T2FLC. Hence T2FLC has an edge of reduced rule base over T1FLC resulting in the simplified design. Moreover, FOU of T2FLC covers identical range of data with few number of labels.

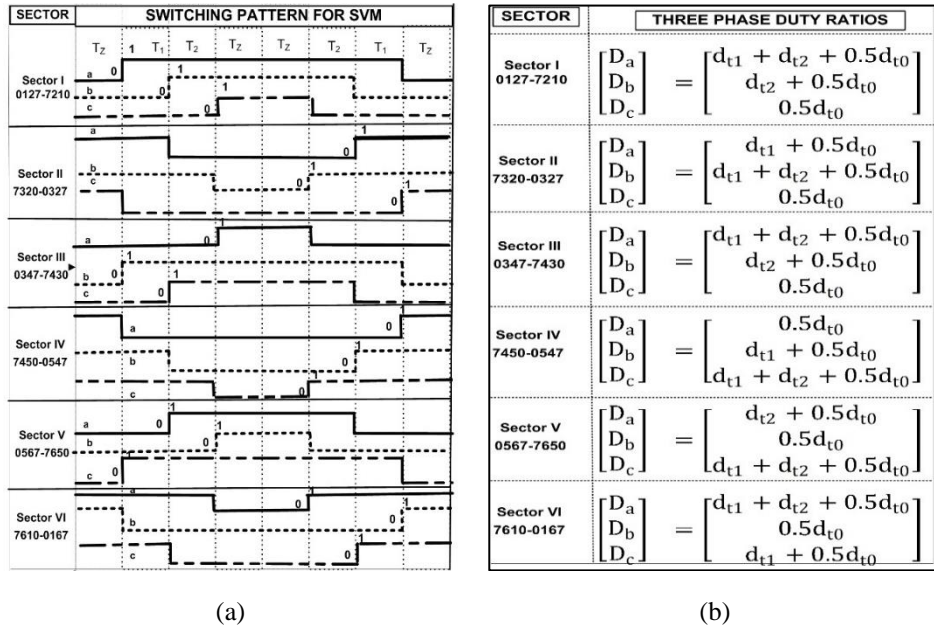


Figure 4. Three phase gate pulse pattern and three phase duty ratios generation in a sequential manner for each sector ($n = 1$ to 6): (a) representation of gate pulse pattern and (b) three phase duty ratios generation

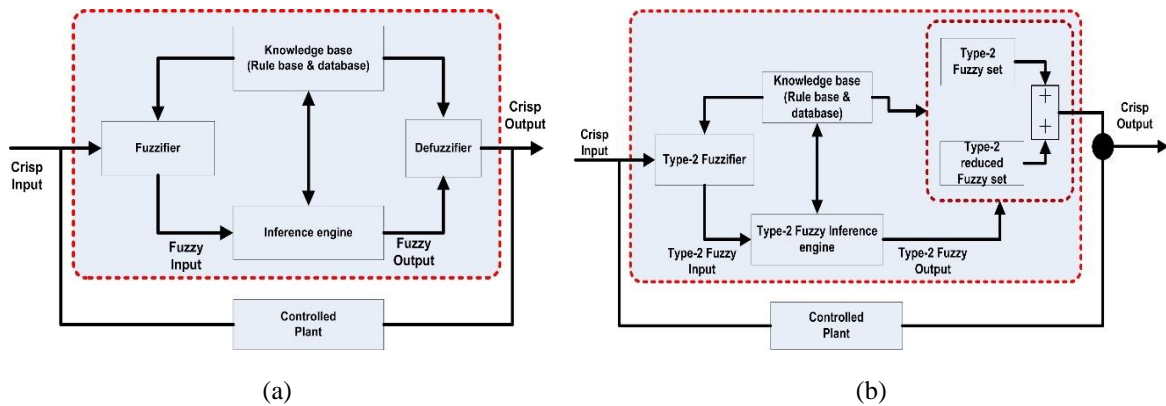


Figure 5. Architecture and description of: (a) type-1 fuzzy system and (b) type-2 fuzzy system

2.2. Type -1 fuzzy logic-based space vector PWM

A crisp output from a T1FLC is obtained by processing input variables through grouping of rules by T1FLC followed by defuzzification. A procedure to choose on which output, or blend of various outputs, will be used is estimated, because each rule could possibly result in a distinct output action. A brief description of membership functions in T1FLC and T2FLC is given in Figure 6. A type-1 fuzzy logic description of the connection between the input and the output can be described by the following illustration. For input premise, 'p' and a particular qualification of the input represented by X_1 , the corresponding output 'u' can be qualified by expression U_1 as indicated in the statement R^1 given in the algorithm form of rules.

- R^1 : IF p is X_1 then u is U_1
- R^2 : IF p is X_2 then u is U_2
- R^n : IF p is X_n then u is U_n

The defuzzification block is used to produces the crisp output value from the T1FLC. The function, in (15) provides a defuzzified value of a MF positioned on associated variable value 'p' using one of the various defuzzification methods, according to the type of argument.

$$A(x) \text{ defuzz}(x, mf, Type) \tag{15}$$

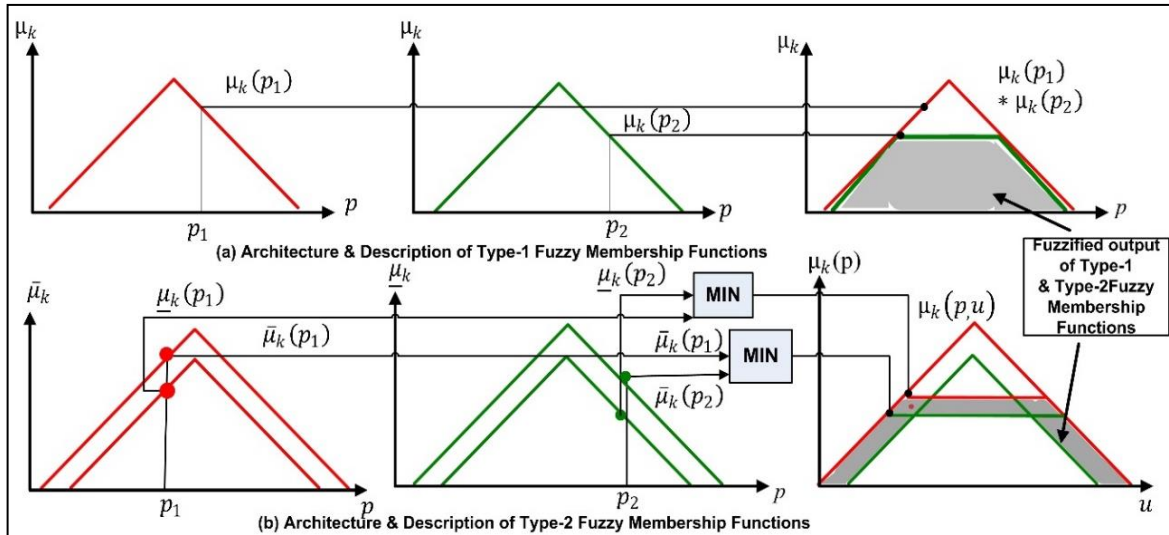


Figure 6. Description of membership functions of type-1 and type-2 fuzzy systems

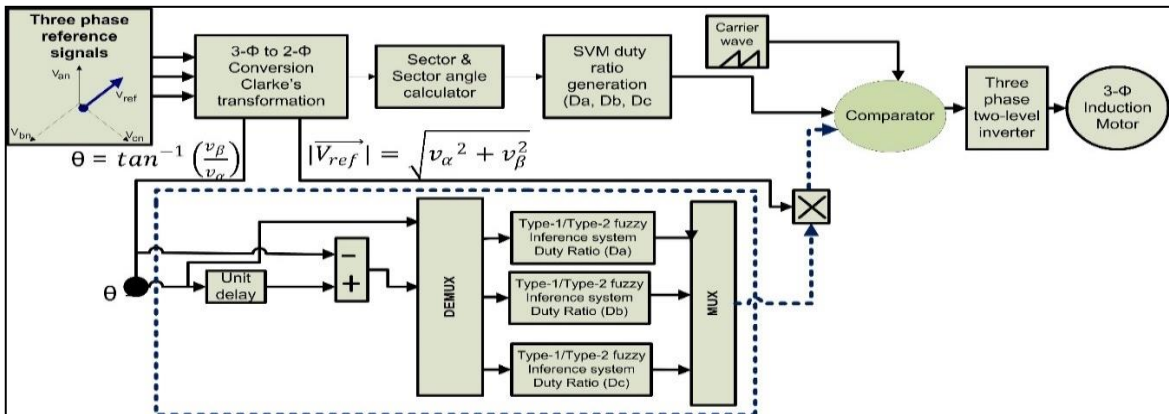


Figure 7. Incorporation of T1FLC and T2FLC in SVM

2.3. Type -2 fuzzy logic-based space vector PWM

The process of a T2FLC is identical with the operation of T1FLC [30]-[33]. However, on the interval type-2 fuzzy system, the fuzzy operation is executed at two type-1 membership functions (MFs) which limits the FOU, i.e., lower MF (LMF) and upper MF (UMF) to produce firing strengths. The additional process of type reduction operation of T2FLC to convert fuzzified type-2 fuzzy set into type-1 fuzzy set is initiated by centre of sets (COS) type reduction technique. Further process of defuzzification is initiated after this step to get crisp output. In COS type reduction operation, interval type-2 fuzzy system is determined by its left most point (LMP) and right most point (RMP) to get to the centroid of interval type-2 consequent set [34]-[36]. A general type-2 fuzzy set \tilde{V} shall be specified by (16).

$$\tilde{V} = \int_{p \in P} \mu_{\tilde{V}}(p) / p = \frac{\int_{p \in P} \left[\int_{\mu \in J_p} \frac{f_p(\mu)}{\mu} \right]}{p} \tag{16}$$

In (16) $\mu_{\tilde{V}}(p)$ is a secondary membership function, J_p is the set of primary membership degrees of $p \in P$ with $\mu \in J_p$ and $f_p(\mu) \in [0,1]$ is a secondary membership degree.

$$\underline{\mu}_{k,i}(p_i) = {}^1\mu_{k,i}(p_i) * {}^2\mu_{k,i}(p_i), k = 1,2, \dots, M, i = 1,2, \dots, n \tag{17}$$

$$\bar{\mu}_{k,i}(p_i) = \bar{\mu}_{k,i}(p_i) = {}^1\mu_{k,i}(p_i) + {}^2\mu_{k,i}(p_i) - \underline{\mu}_{k,i}(p_i) \tag{18}$$

From (17) and (18) $\mu_{k,i}(p_i)$ is the LMF and $\bar{\mu}_{k,i}(p_i)$ is UMF of T2FLC set and they are transformed into a crisp output through the defuzzifier. The operation of T2FLC membership functions is shown in Figure 6. From Figure 7, the sequence of implementing SVM using T1FLC and T2FLC is depicted using dashed lines. The two crisp inputs for the fuzzy logic controllers are phase angle and change in phase angle to generate three phase duty ratios. However, the obtained duty ratios are independent of sampling time and are generated in Figure 8(a) for Da, Figure 8(b) for Db, and Figure 8(c) for Dc respectively at given operating point of IMD. In the designing of rule base seven membership functions ranging between 0 and 1 are applied as given in Figure 8 (a), 8(b) and 8(c) for Da, Db and Dc respectively. The surface view of duty ratios is shown in Figure 9(a) for Da, Figure 9(b) for Db and Figure 9(c) for Dc respectively. The obtained duty cycles are compared with carrier wave to generate switching pulses of two-level inverter as shown in Figure 10(a) SVM, Figure 10(b) type-1 fuzzy SVM, and Figure 10(c) type-2 Fuzzy SVM respectively.

$\Delta\theta_R$ \ θ_R	NH -3.14	NM 2.076	NS -1.047	Z 0.00	PS 1.04	PM 2.09	PH 3.14
Z 0	TA 0.846	TB 0.846	TC 0.846	TD 0.84	TE 0.84	TF 0.84	TA 0.84
PS 0.5	TG 0.9	TG 0.9	TG 0.9	TG 0.9	TG 0.9	TG 0.9	TG 0.9
PM 1	TH 0.854	TH 0.854	TH 0.854	TH 0.84	TH 0.85	TH 0.85	TH 0.85
PH 1.5	TI 0.55	TI 0.55	TI 0.55	TI 0.55	TI 0.55	TI 0.55	TI 0.55
PL 2	TJ 0.22	TJ 0.22	TJ 0.22	TJ 0.22	TJ 0.22	TJ 0.22	TJ 0.22
PL1 2.5	TL 0.1	TL 0.1	TL 0.1	TL 0.1	TL 0.1	TL 0.1	TL 0.1
PL2 3.14	TM 0.153	TN 0.153	TO 0.153	TO 0.15	TP 0.15	TQ 0.15	TR 0.15

(a)

$\Delta\theta_R$ \ θ_R	NL -3.14	NM -2.6	NS -0.52	Z 0	PS 0.52	PM 2.6	PL 3.14
NL -3.14	TA 0.155	TB 0.154	TC 0.154	TD 0.15	TE 0.15	TF 0.15	TA 0.15
NM -2.6	TE 0.485	TE 0.485	TE 0.485	TE 0.485	TF 0.1	TF 0.1	TF 0.1
NS -0.52	TG 0.845	TG 0.845	TG 0.845	TG 0.84	TH 0.15	TH 0.15	TH 0.15
Z 0	TI 0.9	TI 0.9	TI 0.9	TI 0.9	TI 0.1	TJ 0.1	TJ 0.1
PS 0.52	TK 0.846	TK 0.846	TK 0.846	TK 0.84	TL 0.15	TL 0.15	TL 0.15
PM 2.6	TI 0.9	TI 0.9	TI 0.9	TI 0.9	TI 0.42	TJ 0.42	TJ 0.42
PL 3.14	TK 0.846	TK 0.846	TK 0.845	TK 0.84	TK 0.84	TK 0.84	TK 0.84

(b)

$\Delta\theta_R$ \ θ_R	NL -3.14	NM -2.6	NS -0.52	Z 0	PS 0.52	PM 2.6	PL 3.14
NL -3.14	TO 0	TO 0	TC 0.8465	TD 0.8465	TE 0.8464	TF 0.8463	TA 0.8462
NM -2.6	TO 0	TG 0.9	TG 0.9	TG 0.9	TG 0.9	TG 0.9	TG 0.9
NS -0.52	TO 0	TH 0.854	TH 0.854	TH 0.854	TH 0.854	TH 0.854	TH 0.854
Z 0	TO 0	TI 0.55	TI 0.55	TI 0.55	TI 0.55	TI 0.55	TI 0.55
PS 0.52	TO 0	TJ 0.22	TJ 0.22	TJ 0.22	TJ 0.22	TJ 0.22	TJ 0.22
PM 2.6	TO 0	TL 0.1	TL 0.1	TL 0.1	TL 0.1	TL 0.1	TL 0.1
PL 3.14	TO 0	TN 0.1537	TO 0.1535	TO 0.1535	TP 0.1534	TQ 0.1533	TR 0.1532

(c)

Figure 8. Rule base of duty ratios: (a) Da, (b) Db, and (c) Dc of types-1 and type-2 fuzzy based SVM

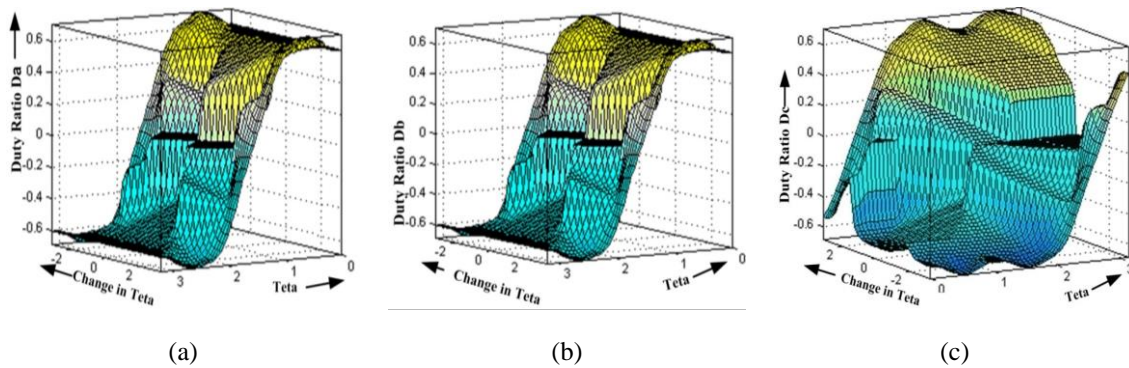


Figure 9. Surface view of duty ratios for three phases a, b, and c: (a) surface view of Dai, (b) surface view of Db, and (c) surface view of Dc

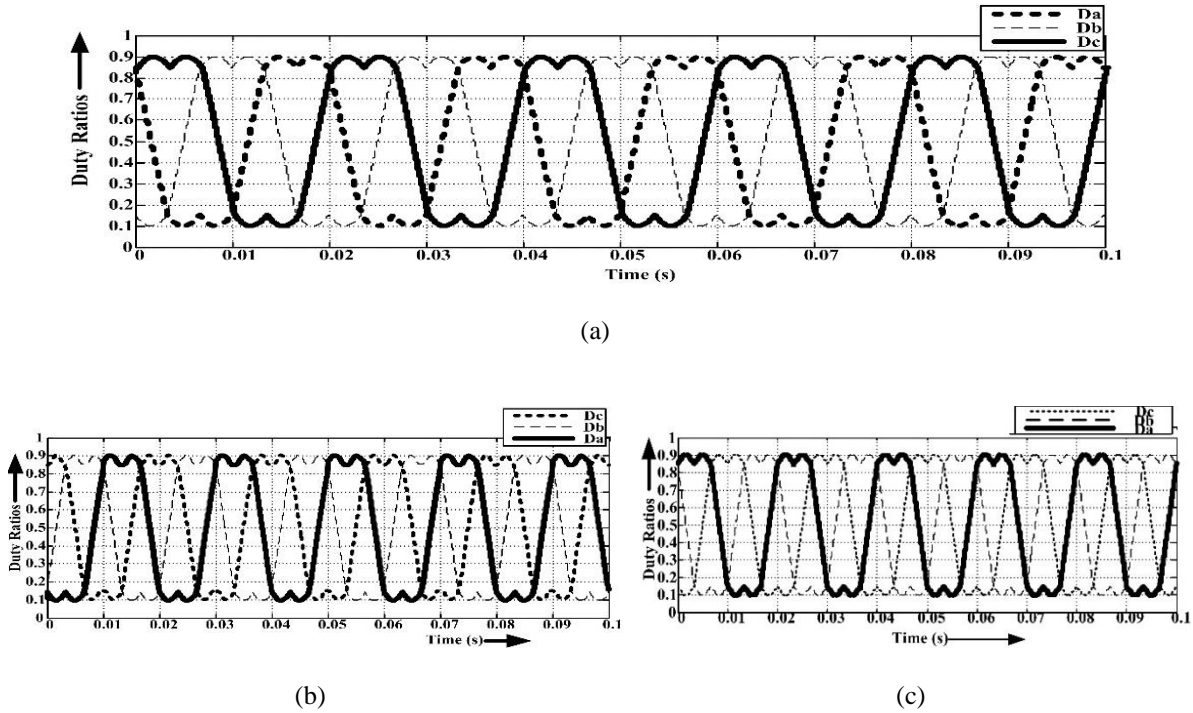


Figure 10. Three phase duty ratios for: (a) SVM, (b) type-1 fuzzy SVM, and (c) type-2 Fuzzy SVM

3. RESULTS AND DISCUSSION

When type-1 and type-2 fuzzy based SVM methods are used in generating three phase duty ratios, after careful investigation of pulse pattern is obtained by proposed methods. Instantaneous voltage vector for SVM is as shown in in Figure 11(a). Figure 11(b) shows instantaneous voltages for type-1 fuzzy SVM and Figure 11(c) shows instantaneous voltages for type-2 fuzzy SVM. An analytical examination on behaviour of pulse pattern when carried out considering a sample case study for switching sequence 0127-7210 clearly reveals underlying reasons for performance improvement. It can be thus inferred that in type-1 and type-2 fuzzy based methods switching sequence is changing at half of carrier cycle or sub-cycle interval for a given sample of reference voltage [35]-[37]. In this case study, when reference voltage is in sector 1, for dc-link voltage $V_{dc} = 400$ V, operating frequency $f = 50$ Hz, switching frequency $f_s = 5$ kHz, and peak value of reference phase voltage vector magnitude $|V_{ref}| = 229$ V is considered with modulation index $m = 0.8$. It is ratio of peak value of reference phase voltage to the fundamental component of square wave. Since $f_s = 5$ kHz, the sampling times $T_s = 200$ μ s and $T_z = 100$ μ s. The discrete step time interval for calculations is $T_d = 10$ μ s. The number of discrete steps for 50 Hz corresponding to time period of $T = 20$ ms is $ns = (T/T_d) = 2000$. Hence number of steps for each sector are $s = (ns/6) = 333.33$ with each step time value of 10 μ s. Now, as $T_s = 200$ μ s number of steps in a carrier wave cycle is given by $nc = (T_s/T_d) = 20$. Also, number of carrier cycles in a sector is given by $ncs = (s \times T_d)/T_s = 16.67$ cycles and 33.34 half carrier cycles. For step time intervals from 0 to 3340 μ s, for all the three case studies instantaneous average voltages are calculated by taking the dwell times using (11) to (14). The proposed types-1 and -2 fuzzy based methods are analytically verified at each sample of reference voltage, the instantaneous value of phase voltage variation with phase angle and is shown in Figure 8. For a given sample over a sub-cycle interval the average value is computed as given in (12) to (14). As the switching pattern is changing in the proposed methods and the instantaneous values are improved close to reference instantaneous phase voltage value. Figure 9 illustrates the three phase voltages pulse pattern in one cycle of reference voltage.

The proposed methods are implemented in real time using STM32F429I ARM Cortex M4 processor. This floating-point unit processor is the latest generation of ARM processors for embedded systems which is a 32-bit micro controller with 180 MHz operating frequency. The performance of the motor is studied at supply frequency of 41 Hz. Hence, motor is operated with reduced dc link voltage $V_{dc} = 400$ V for a modulation index of 0.8 and three phase duty ratios in Figure 10. At this operating condition, instantaneous voltage vector for SVM, type-1 and type-2 fuzzy based methods are given in Figure 11. A close observation indicates increasing dc bus utilization. Additionally, stator current THDs are shown in Figure 12(a) SVM,

Figure 12(b) type-1 fuzzy SVM, and Figure 12(c) type-2 fuzzy SVM. The motor acceleration time is reduced from 0.43 s in space vector PWM (0127) to 0.4 s in type-1 and 0.37 s in type-2 fuzzy based methods as shown in Figure 13(a) SVM, Figure 13(b) type-1 fuzzy SVM, and Figure 13(c) type-2 fuzzy SVM. The experimental set-up is shown in Figure 14. The parameters of IM, inverter details and other accessories are given in Appendix. The test set-up has a three-phase autotransformer fed from three phase supply 3-phase 415 V, 50 Hz, whose output terminals are connected to the three-phase bridge rectifier. Two coupling capacitors C_1 and C_2 are used to filter the dc voltage which is fed as the input for the inverter. The three phases of the output terminals of the inverter are connected through a power analyzer Yokogawa WT-333. The practical THDs for line voltage is 8.162% for SVM as shown in Figure 15(a) for given operating condition, which reduces to 7.852% for type-1 fuzzy based SVM as shown in Figure 15(b) and 6.8% as shown in Figure 15(c) with type-2 fuzzy based SVM. Similarly, the stator current THD is 2.049% for SVM, 1.793% for type-1 and 1.489% for type-2 fuzzy based SVM. To evaluate overall performance of IMD for two different case studies considering seven parameters which include % η of inverter, % η of IM, flux ripple $\Delta\phi_e$ (Wb), electromagnetic torque T_e ripple (Nm), %THD of line voltage (V_L), root mean square (RMS) value of V_L (V) and %THD of line current (I_L) have been investigated at dc link voltage of $V_{dc} = 400$ V and $V_{dc} = 450$ V with a load torque of 1 Nm. The results are included in Table 2 and Table 3. The obtained results indicate that the proposed type-2 fuzzy based SVM improves the performance of IMD when tested rigorously at different operating conditions.

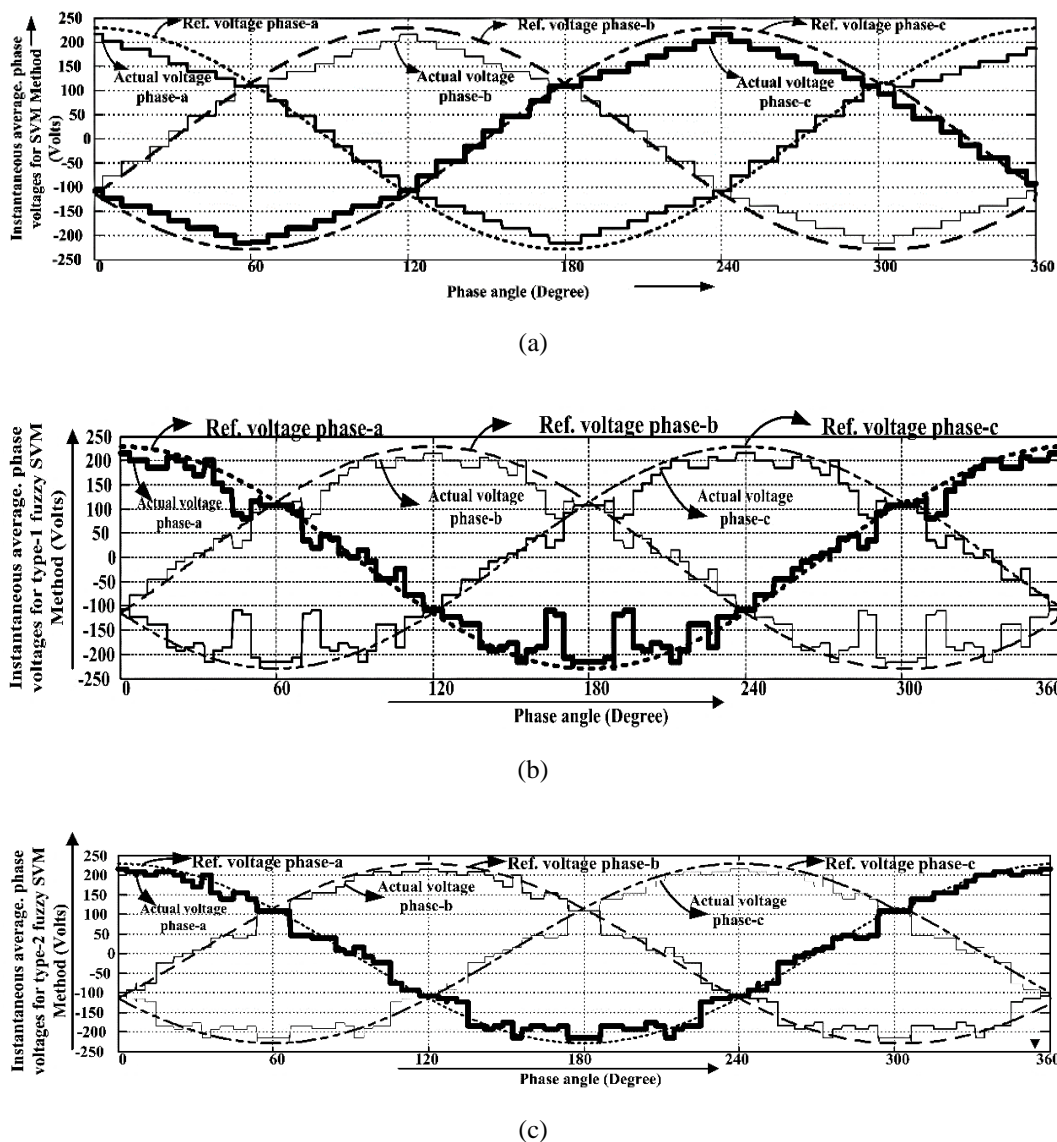


Figure 11. Instantaneous voltage vector for SVM, types-1 and 2 fuzzy: (a) instantaneous voltages for SVM, (b) instantaneous voltages for type-1 fuzzy SVM, and (c) instantaneous voltages for type-2 fuzzy SVM

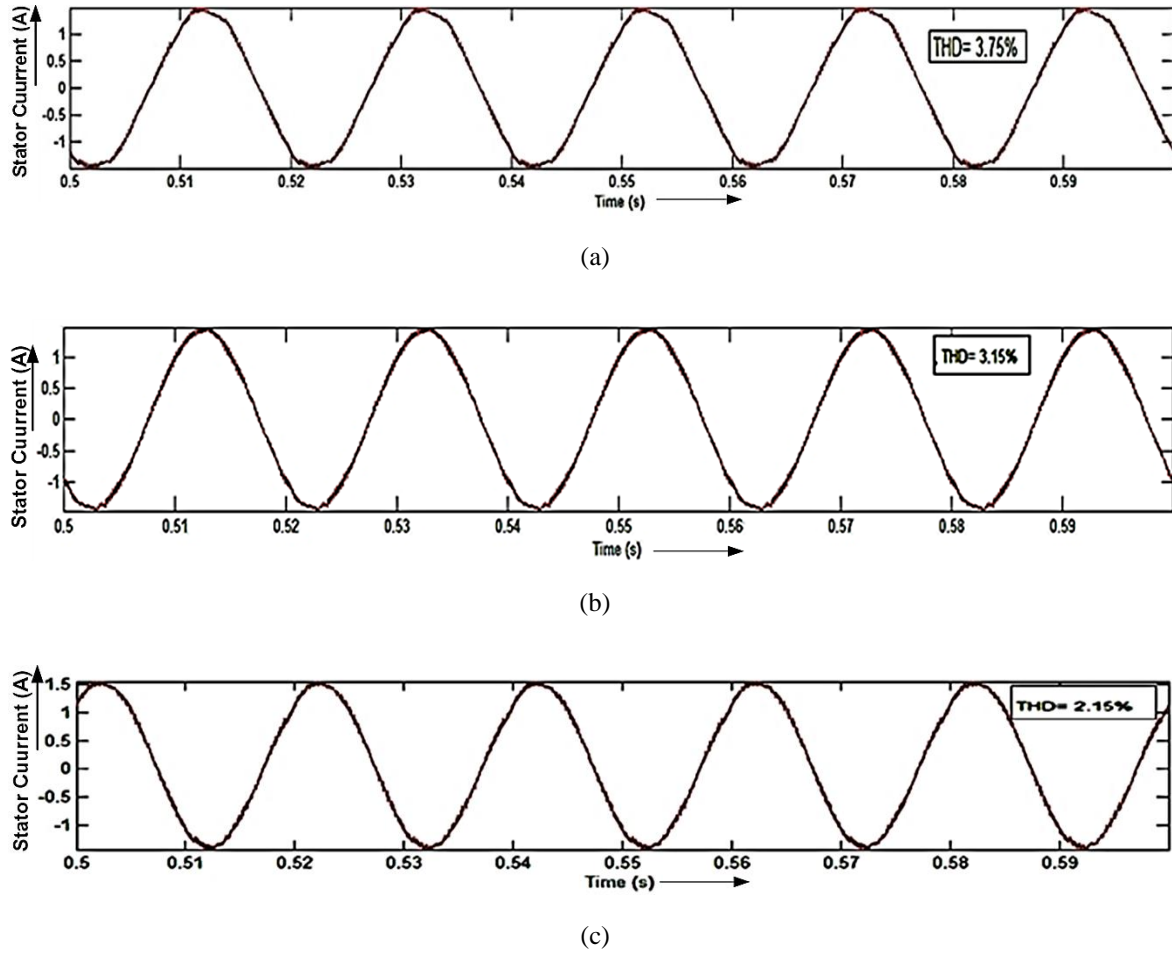


Figure 12. Simulation based stator current THD of: (a) SVM, (b) type-1 fuzzy SVM, and (c) type-2 fuzzy SVM

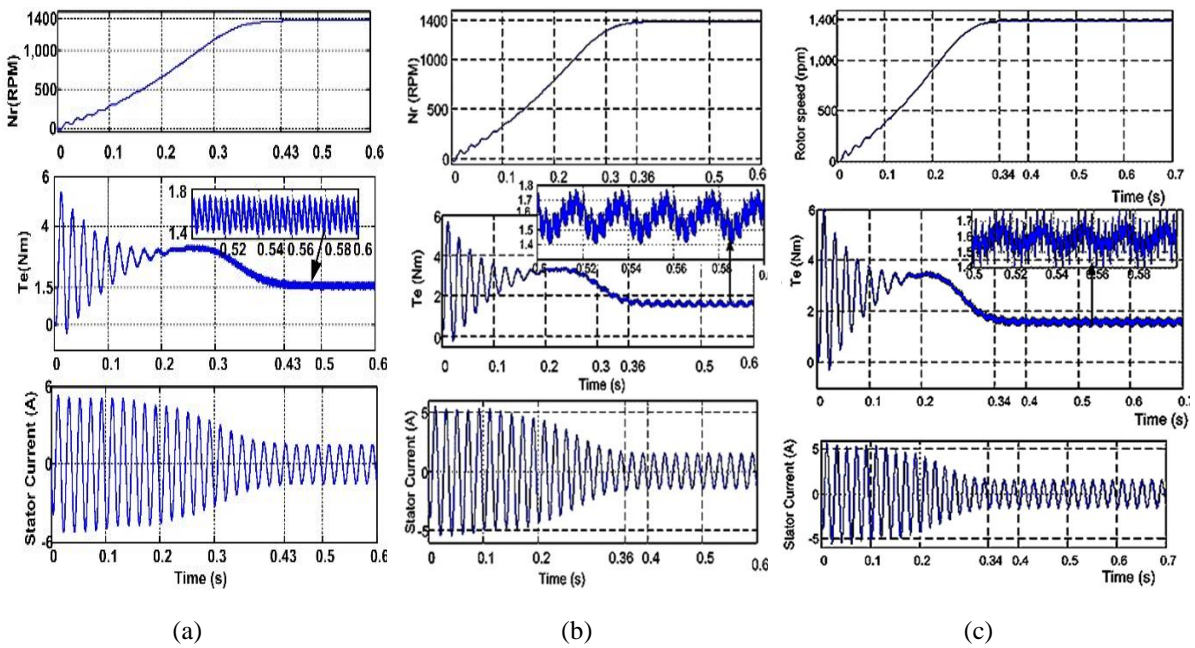


Figure 13. Speed, torque, and stator current of IMD using: (a) SVM, (b) type-1 fuzzy SVM, and (c) type-2 fuzzy SVM

Table 2. Performance evaluation of IMD with dc link voltage of 400 V

Type of SVM	Type-1 fuzzy (m = 0.8)	Type-2 fuzzy (m = 0.8)	Type-1 fuzzy (m = 0.84)	Type-2 fuzzy (m = 0.84)	Type-1 fuzzy (m = 0.866)	Type-2 fuzzy (m = 0.866)
% η of inverter	94.21	97.37	93.22	95.97	92.17	95.11
% η of IM	75.69	77.29	74.28	78.82	81.84	81.84
ϕ_e ripple (Wb)	00.05	00.02	00.06	00.01	00.06	00.05
T_e ripple (Nm)	00.17	00.14	00.19	00.13	00.25	00.08
% THD of V_L	05.80	04.82	06.98	04.27	05.99	04.01
V_L (V)	231.0	260.0	273.7	294.3	301.3	333.5
% THD of I_L	5.748	4.773	5.778	5.376	05.85	5.775

Table 3. Performance evaluation of IMD with dc link voltage of 450 V

Type of SVM	Type-1 fuzzy (m = 0.8)	Type-2 fuzzy (m = 0.8)	Type-1 fuzzy (m = 0.84)	Type-2 fuzzy (m = 0.84)	Type-1 fuzzy (m = 0.866)	Type-2 fuzzy (m = 0.866)
% η of inverter	93.71	93.74	93.70	94.05	94.23	95.34
% η of IM	81.32	87.92	81.38	84.20	86.34	92.58
ϕ_e ripple (Wb)	00.12	00.09	00.05	00.01	0.047	00.04
T_e ripple (Nm)	00.30	00.20	00.24	0.213	0.077	00.03
% THD of V_L	08.30	08.15	07.05	04.99	06.12	04.68
V_L (V)	291.3	327.7	0308	330.3	333.9	339.0
% THD of I_L	6.162	5.076	6.240	5.760	6.680	6.246

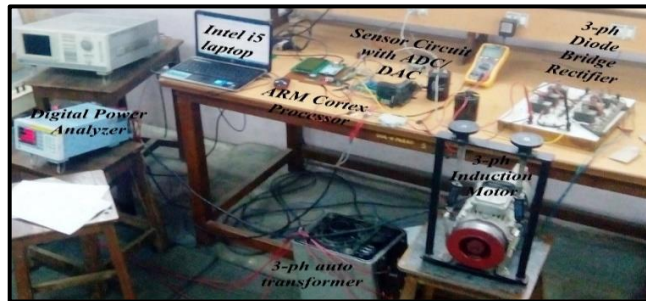


Figure 14. Experimental setup

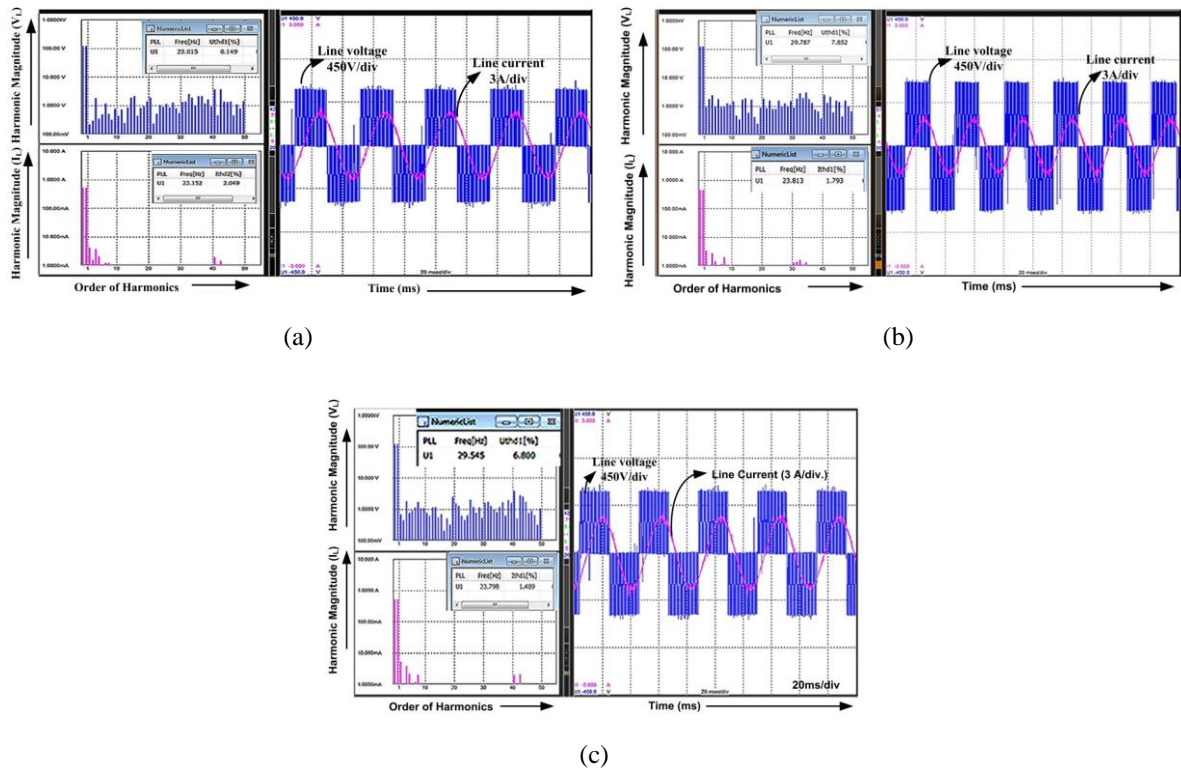


Figure 15. Experiment based comparison of % THDs for (a) SVM, (b) type-1 SVM, and (c) type-2 SVM

4. CONCLUSION

At the inverter end, the transformation of the phase angle and change in phase angle of reference voltage space vector is executed to obtain three phase duty ratios of inverter. This is achieved by using Mamdani non-singleton interval type-1 and type-2 fuzzy inference systems which are designed manually leading to the development of new set of three phases duty ratios which are sampling time independent. Enhanced dc bus utilisation and reduction in THDs of stator voltage and current with improvement in efficiency of IMD is observed with Mamdani based type-1 and type-2 fuzzy based SVM algorithms. The rule base for designing the three phase duty cycles for PWM requires rigorous expertise since several variations occur in duty cycle. Thus, the attained three phase duty cycles can be implemented for any switching frequency with better voltage profile. Further, implementation in hardware using STM32F4 cortex M4 ensures that proposed methods have clear cut edge over conventional SVM.

ACKNOWLEDGEMENTS

The authors would like to acknowledge Mr. K. Vijay Karthik, Department of R&D of Intech DLMS Bengaluru, India for continuous support and encouragement.




REFERENCES

- [1] J. Kennedy and R. Eberhart, "Particle swarm optimization." *Proceedings of ICNN'95 - International Conference on Neural Networks*, 1995, pp. 1942-1948 vol.4, doi: 10.1109/ICNN.1995.488968.
- [2] H. Ma and D. Simon, "Blended biogeography-based optimization for constrained optimization," *Engineering Applications of Artificial Intelligence*, vol. 24, no. 3, pp. 517-525, 2011, doi: 10.1016/j.engappai.2010.08.005.
- [3] Y. Zhang, S. Wang, H. Xia, and J. Ge, "A Novel SVPWM Modulation Scheme," *2009 Twenty-Fourth Annual IEEE Applied Power Electronics Conference and Exposition*, 2009, pp. 128-131, doi: 10.1109/APEC.2009.4802644.
- [4] H. -F. Du, L. -C. Jiao, and S. -A. Wang, "Clonal operator and antibody clone algorithms," *Proceedings International Conference on Machine Learning and Cybernetics*, 2002, pp. 506-510 vol.1, doi: 10.1109/ICMLC.2002.1176807.
- [5] K. M. Passino, "Biomimicry of bacterial foraging for distributed optimization and control," in *IEEE Control Systems Magazine*, vol. 22, no. 3, pp. 52-67, June 2002, doi: 10.1109/MCS.2002.1004010.
- [6] Ş. G. Roşu, C. Rădoi, A. Florescu, P. Guglielmi, and M. Pastorelli, "The analysis of the solutions for harmonic elimination PWM bipolar waveform with a specialized differential evolution algorithm," *2012 13th International Conference on Optimization of Electrical and Electronic Equipment (OPTIM)*, 2012, pp. 814-821, doi: 10.1109/OPTIM.2012.6231900.
- [7] D. Zaharie, "A comparative analysis of crossover variants in differential evolution," in *Proceedings of the International Multiconference on Computer Science and Information Technology (IMCSIT)*, 2007, pp. 171-181. [Online]. Available: <https://citeseerx.ist.psu.edu/viewdoc/download?doi=10.1.1.215.7335&rep=rep1&type=pdf>
- [8] A. Hiendro, "Multiple switching patterns for SHEPWM inverters using differential evolution algorithms," *International Journal of Power Electronics and Drive Systems (IJPEDS)*, vol. 1, no. 2, pp. 94-103, 2011. [Online]. Available: <http://ijpeds.iaescore.com/index.php/IJPEDS/article/view/4867/4256>
- [9] G. Durgasukumarand and M. K. Pathak, "Comparison of adaptive Neuro-Fuzzy-based space-vector modulation for two-level inverter," *International Journal of Electrical Power and Energy Systems*, vol. 38, no. 1, pp. 9-19, 2012, doi: 10.1016/j.ijepes.2011.10.017.
- [10] G. Durgasukumar, T. Abhiram and M. K. Pathak, "TYPE-2 Fuzzy based SVM for two-level inverter fed induction motor drive," *2012 IEEE 5th India International Conference on Power Electronics (IICPE)*, 2012, pp. 1-6, doi: 10.1109/IICPE.2012.6450468.
- [11] V. R. N. Nenavath, S. P. Singh, and A. K. Panda, "An interval type-2 fuzzy-based DTC of IMD using hybrid duty ratio control," *IEEE Transactions on Power Electronics*, vol. 35, no. 8, pp. 8443-8451, Aug. 2020, doi: 10.1109/TPEL.2020.2965722.
- [12] V. R. N. Nenavath, S. P. Singh, A. Panda, and A. K. Panda, "A novel interval type-2 fuzzy-based direct torque control of induction motor drive using five-level diode-clamped inverter," *IEEE Transactions on Industrial Electronics*, vol. 68, no. 1, pp. 149-159, Jan. 2021, doi: 10.1109/TIE.2019.2960738.
- [13] N. V. Naik, J. Thankachan, and S. P. Singh, "A neuro-fuzzy direct torque control using bus-clamped space vector modulation," *IETE Technical Review*, vol. 33, no. 2, pp. 205-217, 2016, doi: 10.1080/02564602.2015.1078750.
- [14] V. M. Deshmukhand and A. J. Patil, "Comparison and performance analysis of closed loop controlled nonlinear system connected PWM inverter based on hybrid technique," *Journal of Electrical Systems and Information Technology*, vol. 2, no. 1, pp. 86-98, 2015, doi: 10.1016/j.jesit.2015.03.008.
- [15] M. S. A. Dahidah, V. G. Agelidis, M. V. Rao, "Hybrid genetic algorithm approach for selective harmonic control," *Energy Conversion and Management*, vol. 49, no. 2, pp. 131-142, 2008, doi: 10.1016/j.enconman.2007.06.031.
- [16] T.-J. Liang, R. M. O'Connell, R. G. Hoft, "Inverter harmonic reduction using walsh function harmonic elimination method," *IEEE Transactions on Power Electronics*, vol. 12, no. 6, pp. 971-982, 1997, doi: 10.1109/63.641495.
- [17] A. K. Al-Othman and T. H. Abdelhamid, "Elimination of harmonics in multilevel inverters with non-equal DC sources using PSO," *2008 13th International Power Electronics and Motion Control Conference*, 2008, pp. 606-613, doi: 10.1109/EPEPEMC.2008.4635332.
- [18] M. Dorigo, V. Maniezzo and A. Colorni, "Ant system: optimization by a colony of cooperating agents," in *IEEE Transactions on Systems, Man, and Cybernetics, Part B (Cybernetics)*, vol. 26, no. 1, pp. 29-41, Feb. 1996, doi: 10.1109/3477.484436.
- [19] K. Sundareswaran, K. Jayant, and T. N. Shanavas, "Inverter Harmonic Elimination Through a Colony of Continuously Exploring Ants," in *IEEE Transactions on Industrial Electronics*, vol. 54, no. 5, pp. 2558-2565, Oct. 2007, doi: 10.1109/TIE.2007.899846.
- [20] T. Ramesh, A. K. Panda, and S. S. Kumar, "Type-2 fuzzy logic control based MRAS speed estimator for speed sensorless direct torque and flux control of an induction motor drive," *ISA transactions*, vol. 57, pp. 262-275, 2015, doi: 10.1016/j.isatra.2015.03.017.
- [21] S. Barkati, E. M. Berkouk, and M. S. Boucherit, "Application of type-2 fuzzy logic controller to an induction motor drive with seven-level diode-clamped inverter and controlled infeed," *Electrical Engineering*, vol. 90, no. 5, pp. 347-359, 2008, doi: 10.1007/s00202-007-0087-x.




- [22] I. Benlaloui, L. C. -Alaoui, M. Ouriagli, A. Khemis, D. Khamari, and S. Drid, "Improvement of the induction motor sensorless control based on the type-2 fuzzy logic," *Electrical Engineering*, vol. 103, no. 3, pp. 1-10, Jun. 2021, doi: 10.1007/s00202-020-01178-1.
- [23] N. V. Naik and S. P. Singh, "Improved torque and flux performance of type-2 fuzzy-based direct torque control induction motor using space vector pulse-width modulation," *Electric Power Components and Systems*, vol. 42, no. 6, pp. 658-669, 2014, doi: 10.1080/15325008.2013.871608.
- [24] T. Abhiram, P. S. Reddy, and P. V. N. Prasad, "Integrated dead-time SVPWM algorithm for indirect vector controlled two-level inverter fed induction motor drive," *2017 International Conference on Information, Communication, Instrumentation and Control (ICICIC)*, 2017, pp. 1-6, doi: 10.1109/ICOMICON.2017.8279073.
- [25] L. A. Zadeh, "Fuzzy sets," in *Information and Control*, vol. 8, pp. 338-353, 1965. [Online]. Available: https://www.liphy.univ-grenoble-alpes.fr/pagesperso/bahram/biblio/Zadeh_FuzzySetTheory_1965.pdf
- [26] T. Takagi and M. Sugeno, "Fuzzy identification of systems and its applications to modeling and control," in *IEEE Transactions on Systems, Man, and Cybernetics*, vol. SMC-15, no. 1, pp. 116-132, Jan.-Feb. 1985, doi: 10.1109/TSMC.1985.6313399.
- [27] S. A. Mir, D. S. Zinger, and M. E. Elbuluk, "Fuzzy controller for inverter fed induction machines," in *IEEE Transactions on Industry Applications*, vol. 30, no. 1, pp. 78-84, Jan.-Feb. 1994, doi: 10.1109/28.273624.
- [28] N. N. Karnik, J. M. Mendel and Qilian Liang, "Type-2 fuzzy logic systems," in *IEEE Transactions on Fuzzy Systems*, vol. 7, no. 6, pp. 643-658, Dec. 1999, doi: 10.1109/91.811231.
- [29] Q. Liang and J. M. Mendel, "Interval type-2 fuzzy logic systems: Theory and design," *IEEE Transactions on Fuzzy Systems*, vol. 8, no. 5, pp. 535-550, Oct. 2000, doi: 10.1109/91.873577.
- [30] S. M. Gadoue, D. Giaouris, and J. W. Finch, "Artificial intelligence-based speed control of DTC induction motor drives-A comparative study," *Electric Power Systems Research*, vol. 79, no. 1, pp. 210-219, 2009, doi: 10.1016/j.eprsr.2008.05.024.
- [31] M. N. Uddin and M. Hafeez, "FLC Based DTC Scheme to Improve the Dynamic Performance of an IM Drive," *2010 IEEE Industry Applications Society Annual Meeting*, 2010, pp. 1-7, doi: 10.1109/IAS.2010.5614089.
- [32] J. M. Mendel, *Uncertain rule-based fuzzy logic systems: Introduction and new directions*, USA: Prentice Hall PTR Book Review, 2001, vol. 133, no. 1, pp. 133-135, doi: 10.1007/978-3-319-51370-6.
- [33] O. Castillo and P. Melin, *Recent advances in interval Type-2 fuzzy systems*, Berlin, Heidelberg, Germany: Springer Science and Business Media, 2012, vol. 1, doi:10.1007/978-3-642-28956-9.
- [34] Y. Xiaoting, Z. Tao, and W. Shasha, "An Interval Type-2 Fuzzy Neural Network Control on Two-Axis Motion System," *TELKOMNIKA Indonesian Journal of Electrical Engineering*, vol. 11, no. 11, pp. 6780-6786, 2013. [Online]. Available: <http://ijeeecs.iaescore.com/index.php/IJEECS/article/view/2836/3964>
- [35] T. Abhiram and P. V. N. Prasad, "Neuro-fuzzy controlled hybrid PWM method for two-level inverter fed three phase induction motor drive," *2016 IEEE International Conference on Power Electronics, Drives and Energy Systems (PEDES)*, 2016, pp. 1-6, doi: 10.1109/PEDES.2016.7914262.
- [36] T. Abhiram and P. V. N. Prasad, "Comparison of fuzzy-2 space vector hybrid PWM method for two-level inverter fed induction motor," *2018 International Conference on Power, Instrumentation, Control and Computing (PICC)*, 2018, pp. 1-6, doi: 10.1109/PICC.2018.8384771.
- [37] A. Tikkani and P. V. N. Prasad, "A Fuzzy-2 Indirect Vector Control of Induction Motor Using Space Vector Fuzzy-2 Based PWM," *Journal of Electrical Engineering & Technology*, vol. 17 pp. 1845-1858, 2022, doi: 10.1007/s42835-022-01021-6.

BIOGRAPHIES OF AUTHORS



Abhiram Tikkani    is currently pursuing Ph.D. from University College of Engineering, Osmania University. He has completed M.E. from University College of Engineering, Osmania University, Hyderabad in 2009. He has more than 15 years of teaching experience and has published over 12 papers in National, IEEE International conferences and international reputed journals. His research interests are in predictive control of ac drives. He was awarded best paper award for his publication in IEEE PEDES 2016. He is a senior Assistant Professor in Sreenidhi Institute of Science and Technology in EEE Department, Hyderabad, India. During his tenure he has guided many M. Tech. projects and is serving as reviewer for reputed international journals. He can be contacted at email: abhiram.cbz@gmail.com.



Polaki V. N. Prasad    graduated in Electrical and Electronics Engg. from Jawaharlal Nehru Technological University, Hyderabad in 1983 and received M.E in Industrial Drives and Control from Osmania University, Hyderabad in 1986. He served as Professor in Dept. of Electrical Engg. and Dean, Faculty of Engg., Osmania University. He received his Ph.D. in Electrical Engg. from Osmania University in 2002. His areas of interest are Simulation of Electrical Machines and Power Electronic Drives and Reliability Engg. He is a fellow of Institution of Engineers India and member in Indian Society for Technical Education. He has got more than 120 publications and over 500 citations in National and International Journals, Conferences and Symposia and presented technical papers in Thailand, Italy, U.S.A and Singapore. He can be contacted at email: pvnprasad09@gmail.com.